Inorg. Chem. **2003**, *42*, 3483–3491

Eilatin as a Bridging Ligand in Ruthenium(II) Complexes: Synthesis, Crystal Structures, Absorption Spectra, and Electrochemical Properties

Dalia Gut, Israel Goldberg, and Moshe Kol*

The School of Chemistry, Raymond and Beverly Sackler Faculty of Exact Sciences, Tel Aviv University, Tel Aviv 69978, Israel

Received December 3, 2002

The potential of the heptacyclic aromatic alkaloid eilatin (**1**), that features two nonequivalent binding sites, to serve as a bridging ligand is reported. The nonequivalency of the binding sites allowed the selective synthesis of both mono- and dinuclear complexes. The mononuclear Ru(II) complexes $[Ru(dmbpy)_2(eilatin)]^{2+}$ (**2**) and $[Ru(tmbpy)_2(eilatin)]^{2+}$ (**3**) in which eilatin selectively binds "head-on" were synthesized and employed as building blocks in the synthesis of the dinuclear complexes $[\{Ru(dmbpy)_2\}_2(\mu\text{-eilatin})]^{4+}$ (**4**) and $[\{Ru(tmbpy)_2\}_2(\mu\text{-eilatin})]^{4+}$ (**5**). Complete structure elucidation of the complexes in solution was accomplished by 1D and 2D NMR techniques. The X-ray structures of the mononuclear complex **3** and of the two dinuclear complexes **4** and **5** were solved, and absorption spectra and electrochemical properties of the complexes were explored. Both dinuclear complexes formed as racemic mixtures in a 3:1 diastereoisomeric ratio, the major isomer being the heterochiral one ($\Delta\Lambda/\Lambda\Delta$) as revealed by crystallography. The mononuclear complexes feature an exceptionally low energy MLCT band around 600 nm that shifted to over 700 nm upon the binding of the second Ru(II) center. The mononuclear complexes show one reversible oxidation and several reversible reduction waves, the first two reductions being substantially anodically shifted in comparison with $[Ru(bpy)_3]^{2+}$, attributed to the reduction of eilatin, and consistent with its low lying π^* orbital. The dinuclear complexes follow the same reduction trend, exhibiting several reversible reduction waves, and two reversible well-resolved metal centered oxidations due to the nonequivalent binding sites and to a significant metal–metal interaction mediated by the bridging eilatin.

Introduction

Dinuclear ruthenium(II) and osmium(II) complexes based on polypyridyl ligands have attracted considerable attention due to their diverse electrochemical and photophysical properties,[1] and possible application in the conversion of solar to electrical energy,[2] in long-range electron and energy transfer[3] and as photoprobes for nucleic acids such as DNA.[4] The bridging ligand, mediating the two metal centers, plays a crucial role in the determination of the properties of these systems. Its structure controls the spatial arrangement, i.e., the distances and relative orientations between the building blocks which constitute the supramolecular array, and the extent of electronic communication between the metal centers, allowing intercomponent energy and electron transfer processes. Planar polyaromatic bridging ligands have been the focus of some recent studies,[5] due to their rigid nature, providing a fixed metal−metal distance and a fully controlled geometry of the resultant array. Although a wide variety of bridging ligands have been introduced in recent years,[1b] the

* To whom correspondence should be addressed. E-mail: moshekol@post.tau.ac.il.

(1) (a) Sauvage, J.-P.; Collin, J.-P.; Chambron, J.-C.; Guillerez, S.; Coudret, C.; Balzani, V.; Barigelletti, F.; De Cola, L.; Flamigni, L. *Chem. Rev.* **1994**, *94*, 993. (b) Balzani, V.; Juris, A.; Venturi, M.; Campagna, S.; Serroni, S. *Chem. Rev.* **1996**, *96*, 759. (c) Balzani, V.; Scandola, F. *Supramolecular Photochemistry*; Ellis Horwood: Chichester, U.K., 1991.

(2) (a) Hagfeldt, A.; Grätzel, M. *Acc. Chem. Res.* **2000**, *33*, 269. (b) Bignozzi, C. A.; Argazzi, R.; Kleverlaan, C. *Chem Soc. Rev.* **2000**, *29*, 87. (c) Meyer, G. J.; Kelly, C. A. *Coord. Chem. Rev.* **2000**, *211*, 295. (d) Kalyanasundaram, K.; Grätzel, M. *Coord. Chem. Rev.* **1998**, *77*, 347.

(3) (a) Collin, J.-P.; Gaviña, P.; Heitz, V.; Sauvage, J.-P. *Eur. J. Inorg. Chem.* **1998**, *1*, 1. (b) Serroni, S.; Campagna, S.; Nascone, R. P.; Hanan, G. S.; Davidson, G. J. E.; Lehn, J.-M. *Chem. Eur. J.* **1999**, *5*, 3523. (c) Barigelletti, F.; Flamigni, L. *Chem. Soc. Rev.* **2000**, *29*, 1. (d) Beyeler, A.; Belser, P. *Coord. Chem. Rev.* **2002**, *230*, 29. (e) De Cola, L.; Belser, P. *Coord. Chem. Rev.* **1998**, *177*, 301.

(4) (a) Foley, F. M.; Keene, F. R.; Collins, G. J. *J. Chem. Soc., Dalton Trans.* **2001**, 2968. (b) Van Gijte, O.; Kirsch-De Mesmaeker, A. *J. Chem. Soc., Dalton Trans.* **1999**, 951. (c) Wilhelmsson, L. M.; Westerlund, F.; Lincoln, P.; Nordén, B. *J. Am. Chem. Soc.* **2002**, *124*, 12092. (d) Patterson, B. T.; Collins, J. G.; Foley, F. M.; Keene, F. R. *J. Chem. Soc., Dalton Trans.* **2002**, 4343.

10.1021/ic020703c CCC: $25.00
Published on Web 04/30/2003

study of dinuclear complexes, bridged by ligands comprised of two nonequivalent binding sites, is less common.[6]

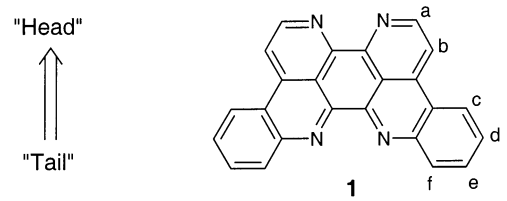

1

Eilatin (**1**) is a heptacyclic planar aromatic alkaloid, originally isolated from a marine organism.[7] This C_{2v} symmetrical compound has two nonequivalent potential binding sites for metals: a bpy type "head" and a biq type "tail" (bpy = 2,2′-bipyridine, biq = 2,2′-biquinoline). We have previously shown[8,9] that eilatin selectively binds metals through its less hindered "head" binding site yielding a variety of mononuclear ruthenium(II) and osmium(II) complexes of the $[M(L-L)_2(eilatin)]^{2+}$ type (L−L = 2,2′-bipyridine, 1,10-phenanthroline, etc.).[10] These complexes feature two unique characteristics: (i) they tend to form discrete dimers held by stacking interactions between the eilatin moieties, in the solid state and in solution, preferably forming heterochiral dimers in racemic mixtures; (ii) they exhibit a markedly low energy metal-to-ligand charge transfer (MLCT) transition attributed to a $d_\pi(Ru) \rightarrow \pi^*$(eilatin) transition due to the low lying π^* orbital of eilatin. Furthermore, it has been recently reported[11] that the eilatin containing metal complexes, Δ- and Λ-$[Ru(bpy)_2(eilatin)]^{2+}$, have significant anti-HIV activities in cell cultures, attributed to the planarity of the eilatin moiety.

In this study, we set forth to explore the potential of eilatin as a rigid nonequivalently bridging ligand, in dinuclear Ru(II) complexes. We report the synthesis, NMR characterization, crystal structures, and electrochemical and spectroscopic properties of the new mononuclear complexes $[Ru(dmbpy)_2(eilatin)]^{2+}$ (**2**) and $[Ru(tmbpy)_2(eilatin)]^{2+}$ (**3**) (dmbpy = 4,4′-dimethyl-2,2′-bipyridine; tmbpy = 4,4′,5,5′-tetramethyl-2,2′-bipyridine) and their consequent dinuclear complexes, $[\{Ru(dmbpy)_2\}_2(\mu\text{-eilatin})]^{4+}$ (**4**) and $[\{Ru(tmbpy)_2\}_2(\mu\text{-eilatin})]^{4+}$ (**5**).

Experimental Section

Materials. Eilatin (**1**),[12] tmbpy,[13] *rac*-$[Ru(bpy)_2(eilatin)][PF_6]_2$ (**6**),[8] *cis*-$[Ru(dmbpy)_2Cl_2]$,[14] and *cis*-$[Ru(tmbpy)_2Cl_2]$[14] were synthesized according to literature procedures. Tetrabutylammonium hexafluorophosphate (98%) and silver nitrate (99.995%) were purchased from Aldrich and used without further purification. All other chemicals and solvents used were of reagent grade and used without further purification, except acetonitrile (for electrochemical measurements) which was distilled over CaH_2. All the reactions and electrochemical measurements were performed under an argon atmosphere.

Instrumentation. ^1H and ^{13}C NMR spectra and COSY, NOESY, and HMQC experiments were performed with a Bruker Avance 400 spectrometer using the residual protons of the solvent (CD_3CN) as an internal standard at $\delta = 1.93$ ppm. UV−vis absorption spectra in acetonitrile were obtained with a Kontron UVIKON 931 UV−vis spectrometer. FABMS data were obtained on a VG-AutoSpec M250 mass spectrometer, in a *m*-nitrobenzyl alcohol matrix. Cyclic and square wave voltammograms were carried out on a μ-autolab type II potentiostat (Eco Chemie), using a platinum working electrode, a platinum auxiliary electrode, and a $Ag/AgNO_3$ (0.01 M in acetonitrile) reference electrode (BAS). The measurements were carried out on the complexes dissolved in argon-purged acetonitrile containing 0.1 M tetabutylammonium hexafluorophosphate (TBAH) as supporting electrolyte. The typical concentration of the complexes was ca. 1.5 mM. The criteria for reversibility were the separation between the cathodic and anodic peaks, the close-to-unity ratio of the intensities of the cathodic and anodic peak currents, and the constancy of the peak potential on changing scan rate. A 5 mM solution of ferrocene in acetonitrile containing 0.1 M TBAH was measured after the measurement of each complex, typically yielding a value of $E_{1/2} = 0.096$ V for Fc/Fc^+. Values were converted to the SCE scale assuming $E_{1/2} = 400$ mV for Fc/Fc^+.[15]

Synthesis. $[Ru(dmbpy)_2(eilatin)][PF_6]_2$ (2). *rac,cis*-$[Ru(dmbpy)_2Cl_2]$ (50 mg, 0.093 mmol) and eilatin (39 mg, 0.109 mmol) were dissolved in 20 mL of a 4:1 methanol−water solution and refluxed for 5 h. The resultant green reaction mixture was cooled, and the solvent was evaporated. The green complex was then redissolved in a minimal amount of methanol for purification using a column of Sephadex LH-20 as support and methanol as eluent. The major bluish-green product band was collected, concentrated by evaporation to ca. 3 mL, and precipitated by the addition of a saturated aqueous solution of KPF_6. The mixture was filtered, and the complex was washed twice with 5 mL of H_2O. The complex was further purified by recrystallization by a slow evaporation of an acetonitrile−toluene solution. Typical yield was 95%. Anal. Calcd (Found) for $C_{48}H_{36}F_{12}N_8P_2Ru\cdot 2H_2O\cdot 0.5C_7H_8$: C, 52.42 (52.44); H, 3.59 (4.21); N, 9.50 (9.15). ^1H NMR (CD_3CN, 9.3 ×

(5) (a) Bolger, J.; Gourdon, A.; Ishow, E.; Launay, J.-P. *Inorg. Chem.* **1996**, *35*, 2937. (b) Gourdon, A.; Launay, J.-P. *Inorg. Chem.* **1998**, *37*, 5336. (c) Ishow, E.; Gourdon, A.; Launay, J.-P. *Chem. Commun.* **1998**, 1909. (d) Ishow, E.; Gourdon, A.; Launay, J.-P.; Chiorboli, C.; Scandola, F. *Inorg. Chem.* **1999**, *38*, 1504. (e) Bolger, J.; Gourdon, A.; Ishow, E.; Launay, J.-P. *J. Chem. Soc., Chem. Commun.* **1995**, 1799. (f) Bilakhiya, A. K.; Tyagi, B.; Parimal, P.; Natarjan, P. *Inorg. Chem.* **2002**, *41*, 3830. (g) Kim, M.-J.; Konduri, R.; Ye, H.; MacDonnell, F. M.; Puntoriero, F.; Serroni, S.; Campagna, S.; Holder, T.; Kinsel, G.; Rajeshwar, K. *Inorg. Chem.* **2002**, *41*, 2471. (h) Thummel, R. P.; Williamson, D.; Hery, C. *Inorg. Chem.* **1993**, *32*, 1587.

(6) (a) Balzani, V.; Bardwell, D. A.; Barigelletti, F.; Cleary, R. L.; Guardigli, M.; Jeffery, J. C.; Sovrani, T.; Ward, M. D. *J. Chem. Soc., Dalton Trans.* **1995**, 3601. (b) Hage, R.; Haasnoot, J. G.; Nieuwenhuis, H. A.; Reedijk, J.; De Ridder, D. J. A.; Vos, J. G. *J. Am. Chem. Soc.* **1990**, *112*, 5. (c) Fletcher, N. C.; Robinson, T. C.; Behrendt, A.; Jeffery, J. C.; Reeves, Z. R.; Ward, M. D. *J. Chem. Soc., Dalton Trans.* **1999**, 2999. (d) Komatsuzaki, N.; Kotoh, R.; Himeda, Y.; Sugihara, H.; Arakawa, H.; Kasuga, K. *J. Chem. Soc., Dalton Trans.* **2000**, 3053.

(7) Rudi, A.; Benayahu, I.; Goldberg, I.; Kashman, Y. *Tetrahedron Lett.* **1988**, *29*, 6655.

(8) Rudi, A.; Kashman, Y.; Gut, D.; Lellouche, F.; Kol, M. *Chem. Commun.* **1997**, 17.

(9) Gut D.; Rudi, A.; Kopilov, J.; Goldberg, I.; Kol, M. *J. Am. Chem. Soc.* **2002**, *124*, 5449.

(10) Mononuclear "head-bound" eilatin complexes of the $[M(L-L)(eilatin)_2]^{2+}$ and $[M(eilatin)_3]^{2+}$ types have been prepared as well and will be reported in due course.

(11) Luedtke, N. W.; Hwang, J. S.; Glazer, E. C.; Gut, D.; Kol, M.; Tor, Y. *ChemBioChem* **2002**, *3*, 766.

(12) Gellerman, G.; Rudi, A.; Kashman, Y. *Tetrahedron* **1994**, *50*, 12959.

(13) Patterson, B. T.; Keene, F. R. *Inorg. Chem.* **1998**, *37*, 645.

(14) Sullivan, B. P.; Salmon, D. J.; Meyer, T. J. *Inorg. Chem.* **1978**, *17*, 3334.

(15) Connelly, N. G.; Geiger, W. E. *Chem. Rev.* **1996**, *96*, 877. (Fc/Fc^+ vs SCE.)

10^{-4} M, 298 K): δ 8.71 (d, $J = 8.0$ Hz, 1H, H^c), 8.51 (d, $J = 6.4$ Hz, 1H, H^b), 8.42 (s, 1H, H^3), 8.36 (s, 1H, $H^{3'}$), 8.31 (d, $J = 8.1$ Hz, 1H, H^f), 8.14 (d, $J = 6.4$, 1H, H^a), 8.08 (d, $J = 7.3$ Hz, 1H, H^e), 7.97 (t, $J = 7.4$ Hz, 1H, H^d), 7.65 (d, $J = 5.8$, 1H, H^6), 7.60 (d, $J = 5.8$ Hz, 1H, $H^{6'}$), 7.36 (d, $J = 5.6$ Hz, 1H, H^5), 7.11 (d, $J = 5.9$ Hz, 1H, $H^{5'}$), 2.61 (s, 3H, CH_3), 2.45 (s, 1H, CH_3'). ^{13}C NMR: δ 153.2 (*C*-$H^{6'}$), 151.6 (*C*-H^6), 150.3 (*C*-H^a), 134.0 (*C*-H^e), 132.7 (*C*-H^f), 131.2 (*C*-H^d), 129.4 (*C*-H^5), 129.2 (*C*-$H^{5'}$), 125.9 (*C*-H^3), 125.6 (*C*-$H^{3'}$), 124.8 (*C*-H^c), 122.1 (*C*-H^b), 21.2 (*C*-H_3), 21.1 (*C*-H_3'). FABMS: 826 $[M - 2PF_6]^+$, 971 $[M - PF_6]^+$.

[Ru(tmbpy)$_2$(eilatin)][PF$_6$]$_2$ (3). This complex was prepared and purified by the same method described for **2**, utilizing *rac,cis*-[Ru(tmbpy)$_2$Cl$_2$] (50 mg, 0.084 mmol) and eilatin (37 mg, 0.104 mmol). Typical yield was 90%. Anal. Calcd (Found) for $C_{52}H_{44}F_{12}N_8P_2Ru{\cdot}2H_2O$: C, 51.70 (51.72); H, 4.01 (4.21); N, 9.28 (9.34). ^{1}H NMR (CD_3CN, 9.5×10^{-4} M, 298 K): δ 8.61 (d, $J = 8.1$ Hz, 1H, H^c), 8.44 (d, $J = 6.4$ Hz, 1H, H^b), 8.33 (s, 1H, H^3), 8.26 (s, 1H, $H^{3'}$), 8.13 (d, $J = 6.4$ Hz, 2H, H^a, H^f), 8.01 (t, $J = 7.5$ Hz, 1H, H^e), 7.92 (t, $J = 7.2$ Hz, 1H, H^d), 7.47 (s, 1H, H^6), 7.44 (s, 1H, $H^{6'}$), 2.54 (s, 3H, $CH_3{}^4$), 2.37 (s, 3H, $CH_3{}^{4'}$), 2.20 (s, 1H, $CH_3{}^5$), 1.95 (s, 1H, $CH_3{}^{5'}$). ^{13}C NMR: δ 152.2 (*C*-$H^{6'}$), 150.9 (*C*-H^6), 150.2 (*C*-H^a), 132.2 (*C*-H^f), 131.7(*C*-H^e), 130.8 (*C*-H^d), 125.3 (*C*-H^3), 125.0 (*C*-$H^{3'}$), 124.6 (*C*-H^c), 121.7 (*C*-H^b), 19.5 (*C*-$H_3{}^4$), 19.3 (*C*-$H_3{}^{4'}$), 16.8 (*C*-$H_3{}^5$), 16.5 (*C*-$H_3{}^{5'}$). FABMS: 882 $[M - 2PF_6]^+$, 1027 $[M - PF_6]^+$.

[{Ru(dmbpy)$_2$}$_2$(μ-eilatin)][PF$_6$]$_4$ (4). *rac,cis*-[Ru(dmbpy)$_2$Cl$_2$] (38 mg, 0.070 mmol) and [Ru(dmbpy)$_2$(eilatin)][Cl]$_2$ (50 mg, 0.056 mmol) were dissolved in 7 mL of deoxygenated ethylene glycol. The reaction mixture was heated in a 50 mL pressure vessel at 140 °C for 32 h. The resultant green reaction mixture was cooled and the crude product precipitated by the addition of a saturated aqueous solution of KPF_6. The mixture was filtered, and the resultant green solid was washed twice with 5 mL of H_2O. Purification was achieved by cation exchange chromatography (CM sephadex C-25; eluent 5:3 MeOH/NaCl 0.1−0.5 M). The green-yellow band was collected, concentrated by evaporation to ca. 10 mL, and precipitated by the addition of a saturated aqueous solution of KPF_6. The precipitate was collected, washed twice with 5 mL of H_2O, and dried in vacuo. Yield 67%. The complex was dissolved in 4 mL of acetonitrile, and 3 mL of toluene was slowly added. After 3 days in which the solution was allowed to slowly evaporate, dark green square crystals together with a few long needle-shaped crystals separated from the solution. The crystals were separated from the solution, and repeated crystallization by the described method yielded the heterochiral ($\Delta\Lambda/\Lambda\Delta$) diastereoisomers (determined by X-ray crystallography). Anal. Calcd (Found) for $C_{72}H_{60}F_{24}N_{12}P_4Ru_2{\cdot}2H_2O$: C, 45.24 (45.59); H, 3.38 (3.71); N, 8.79 (8.88). ^{1}H NMR for the $\Delta\Lambda/\Lambda\Delta$ isomers (CD_3CN, 300 K): δ 8.86 (d, $J = 7.9$ Hz, 1H, H^c), 8.76 (d, $J = 6.4$ Hz, 1H, H^b), 8.44 (s, 1H, H^{3h}), 8.36 (m, 3H, H^a, $H^{3h'}$, H^{3t}), 8.24 (s, 1H, $H^{3t'}$), 7.93 (t, $J = 7.4$ Hz 1H, H^d), 7.69 (d, $J = 5.7$ Hz, 1H, H^{6h}), 7.64 (d, $J = 5.8$ Hz, 1H, H^{6t}), 7.50 (t, $J = 7.7$ Hz, 1H, H^e), 7.47 (d, $J = 5.9$ Hz, 1H, $H^{6h'}$), 7.37 (m, 3H, H,^{5h} H^f, H^{5t}), 7.22 (d, $J = 5.7$ Hz, 1H, $H^{6t'}$), 7.13 (d, $J = 5.1$ Hz, 1H, $H^{5h'}$), 7.00 (d, $J = 5.1$ Hz, 1H, $H^{5t'}$), 2.62 (s, 3H, $CH_3{}^{4h}$), 2.58 (s, 3H, $CH_3{}^{4t}$), 2.47 (s, 3H, $CH_3{}^{4h'}$), 2.38 (s, 3H, $CH_3{}^{4t'}$). ^{13}C NMR: δ 153.1 (*C*-$H^{6t'}$), 152.6 (*C*-$H^{6h'}$), 152.5 (*C*-H^a), 151.3 (*C*-H^{6h}), 151.2 (*C*-H^{6t}), 132.3 (*C*-H^d), 129.8 (*C*-$H^{5t'}$), 129.7 (*C*-H^{5h}), 129.5 (*C*-H^{5t}), 129.5 (*C*-H^e), 129.2 (*C*-$H^{5h'}$), 126.8 (*C*-H^f), 126.7 (*C*-H^c), 126.3 (*C*-$H^{3t'}$), 126.2 (*C*-H^{3t}), 126.1 (*C*-$H^{3h'}$), 126.1 (*C*-H^{3h}), 121.9 (*C*-H^b), 21.2 (*C*-$H_3{}^{4h}$), 21.2 (*C*-$H_3{}^{4t}$), 21.0 (*C*-$H_3{}^{4h'}$), 21.0 (*C*-$H_3{}^{4t'}$). FABMS: 1440 $[M - 3PF_6]^+$, 1586 $[M - 2PF_6 + H]^+$, 1730 $[M - PF_6]^+$.

[{Ru(tmbpy)$_2$}$_2$(μ-eilatin)][PF$_6$]$_4$ (5). This complex was prepared and purified by the same method described for **4**, utilizing *rac,cis*-[Ru(tmbpy)$_2$Cl$_2$] (40 mg, 0.067 mmol) and [Ru(tmbpy)$_2$(eilatin)][Cl]$_2$ (50 mg, 0.052 mmol). Yield 95%. The complex was dissolved in 4 mL of acetonitrile, and 3 mL of toluene was slowly added. After 3 days in which the solution was allowed to slowly evaporate, dark green square crystals together with a few long needle-shaped crystals separated from the solution. The crystals were separated from the solution, and repeated crystallization by the described method yielded the heterochiral ($\Delta\Lambda/\Lambda\Delta$) diastereoisomers (determined by X-ray crystallography). Anal. Calcd (Found) for $C_{80}H_{76}F_{24}N_{12}P_4Ru_2{\cdot}H_2O$: C, 47.91 (47.62); H, 3.92 (4.04); N, 8.38 (8.60). ^{1}H NMR for the $\Delta\Lambda/\Lambda\Delta$ isomers (CD_3CN, 300 K): δ 8.86 (d, $J = 8.0$ Hz, 1H, H^c), 8.76 (d, $J = 6.4$ Hz, 1H, H^b), 8.36 (d, $J = 6.4$ Hz, 1H, H^a), 8.34 (s, 1H, H^{3h}), 8.25 (s, 1H, $H^{3h'}$), 8.23 (s, 1H, H^{3t}), 8.11 (s, 1H, $H^{3t'}$), 7.92 (t, $J = 7.4$ Hz, 1H, H^d), 7.44 (m, 4H, H^e, H^f, H,^{6h}H^{6t}), 7.18 (s, 1H, $H^{6h'}$), 6.98 (s, 1H, $H^{6t'}$), 2.53 (s, 3H, $CH_3{}^{4h}$), 2.49 (s, 3H, $CH_3{}^{4t}$), 2.38 (s, 3H, $CH_3{}^{4h'}$), 2.27 (s, 3H, $CH_3{}^{4t'}$), 2.19 (s, 3H, $CH_3{}^{5h}$), 2.13 (s, 3H, $CH_3{}^{5t}$), 1.93 (s, 3H, $CH_3{}^{5h'}$), 1.72 (s, 3H, $CH_3{}^{5t'}$). ^{13}C NMR: δ 152.8 (*C*-$H^{6t'}$), 152.6 (*C*-H^a), 152.5 (*C*-$H^{6h'}$), 151.0 (*C*-H^{6h}), 150.7 (*C*-H^{6t}), 133.8 (*C*-H^e), 132.1 (*C*-H^d), 127.2 (*C*-H^f), 126.4 (*C*-H^c), 125.5 (*C*-H^{3h}), 125.4 (*C*-$H^{3t'}$), 125.3 (*C*-$H^{3h'}$), 125.3 (*C*-H^{3t}), 121.7 (*C*-H^b), 19.8 (*C*-$H_3{}^{4h}$), 19.6 (*C*-$H_3{}^{4t}$), 19.5 (*C*-$H_3{}^{4h'}$), 19.4 (*C*-$H_3{}^{4t'}$), 17.1 (*C*-$H_3{}^{5h'}$), 17.0 (*C*-$H_3{}^{5h}$), 17.0 (*C*-$H_3{}^{5t}$), 16.8 (*C*-$H_3{}^{5t'}$). FABMS: 848 $[M - 2PF_6]^{2+}$, 1553 $[M - 3PF_6 + H]^+$, 1697 $[M - 2PF_6]^+$, 1842 $[M - PF_6]^+$.

X-ray Structure Determinations. The X-ray diffraction measurements were carried out at ca. 110 K on a Nonius Kappa CCD diffractometer, using Mo Kα ($\lambda = 0.7107$ Å) radiation. Single crystals of these compounds could be grown only as toluene and acetonitrile solvates. The analyzed crystals were embedded within a drop of an amorphous viscous oil and freeze-cooled to 110 K, in order to minimize deterioration, lower the thermal motion and structural disorder effects, and improve the precision of the results. The crystal structures were solved by Patterson and Fourier techniques (DIRDIF-96)[16] and refined by full-matrix least-squares (SHELXL97).[17]

Crystal Data for 3. $C_{52}H_{44}F_{12}N_8P_2Ru{\cdot}C_7H_8$, formula weight 1264.10, monoclinic, space group $C2/c$, $a = 36.3060(9)$ Å, $b = 14.7720(4)$ Å, $c = 21.2170(7)$ Å, $\beta = 102.202(2)°$, $V = 11121.9(5)$ Å^3, $Z = 8$, $D_{calcd} = 1.510$ g·cm^{-3}, $F(000) = 5152$, μ(Mo Kα) = 4.28 cm^{-1}, $2\theta_{max} = 50.0°$, 9657 unique reflections. R1 = 0.068 (wR2 = 0.180) for 6521 reflections with $F_o > 4\sigma(F_o)$, and R1 = 0.111 (wR2 = 0.211) for all data. Two of the PF_6 anions are located at special positions on axes of twofold rotational symmetry. The toluene solvent is severely disordered.

Data for 4. $C_{72}H_{60}F_{24}N_{12}P_4Ru_2$ (excluding solvent), formula weight 1875.34, monoclinic, space group $P2_1/c$, $a = 17.7620(4)$ Å, $b = 25.3500(8)$ Å, $c = 21.0750(6)$ Å, $\beta = 96.696(3)°$, $V = 9424.6(5)$ Å^3, $Z = 4$, $D_{calcd} = 1.322$ g.cm^{-3}, $F(000) = 3760$, μ(Mo Kα) = 4.78 cm^{-1}, $2\theta_{max} = 51.3°$, 17004 unique reflections. R1 = 0.123 (wR2 = 0.268) for 7730 reflections with $F_o > 4\sigma(F_o)$, and R1 = 0.241 (wR2 = 0.301) for all data. The analyzed crystals were characterized by high mosaic spread. They contain disordered/diffused (toluene) solvent which could not be properly modeled. The PF_6 anions, as well as several fragments of the main molecular framework, are partly disordered as well. Correspondingly, the data

(16) Beurskens, P. T.; Beurskens, G.; Bosman, W. P.; de Gelder, R.; Garcia-Granda, S.; Gould, R. O.; Israel, R.; Smits, J. M. M. *DIRDIF-96*; Crystallography Laboratory, University of Nijmegen: Nijmegen, The Netherlands, 1996.

(17) Sheldrick, G. M. *SHELXL-97. Program for the Refinement of Crystal Structures from Diffraction Data*; University of Göttingen: Göttingen, Germany, 1997.

Scheme 1. Synthesis of Mono- and Dinuclear Complexes of Eilatin **2**−**5**

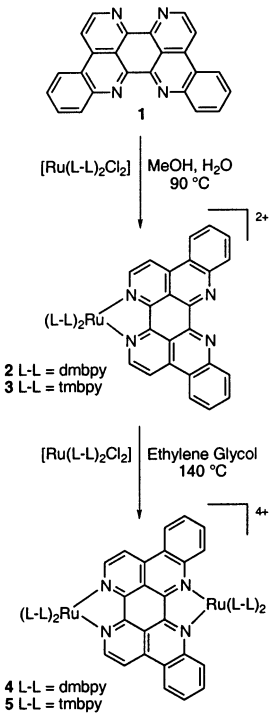

set contains a large fraction of very weak reflections below the intensity threshold of $2\sigma(I)$. While the resulting precision of this determination is relatively poor (as it is commonly observed in related compounds),[18−20] it still describes reasonably well the connectivity and main structural features of this dinuclear complex.

Data for 5. $C_{80}H_{76}F_{24}N_{12}P_4Ru_2 \cdot CH_3CN \cdot 4(C_7H_8)$, formula weight 2393.11, triclinic, space group $P\bar{1}$, $a = 17.107(1)$ Å, $b = 18.353(1)$ Å, $c = 21.814(1)$ Å, $\alpha = 65.01(1)°$, $\beta = 83.84(1)°$, $\gamma = 69.83(1)°$, $V = 5820.8(5)$ Å^3, $Z = 2$, $D_{calcd} = 1.365$ g·cm^{-3}, $F(000) = 2444$, μ(Mo Kα) = 4.03 cm^{-1}, $2\theta_{max} = 50.0°$, 18425 unique reflections. R1 = 0.074 (wR2 = 0.200) for 12312 reflections with $F_o > 4\sigma(F_o)$, and R1 = 0.118 (wR2 = 0.233) for all data. The asymmetric unit contains four PF_6 ions (suffering from partial orientation disorder), one molecule of acetonitrile, and several disordered moieties of toluene solvent.

Results

Syntheses. The reaction between $[Ru(L-L)_2Cl_2]$ (L−L = dmbpy or tmbpy) and excess eilatin in refluxing aqueous methanol yields the mononuclear complexes **2** and **3**, respectively, of "head" bound eilatin in good selectivity[8] and in high yields (Scheme 1). A dinuclear species is not formed, due to the relatively mild reaction conditions applied, and to the utilization of an excess of eilatin. The complexes were purified by gel permeation chromatography, using a column of Sephadex LH-20 as support and methanol as eluent, and were then used as precursors for the synthesis of the dinuclear complexes. The complexes were metathesized, for characterization purposes, to their hexafluorophosphate salts, by the addition of a saturated aqueous solution of KPF_6 to a concentrated methanol solution of each complex.

The synthesis of the dinuclear complexes **4** and **5** could be achieved by employing more drastic reaction conditions (Scheme 1). Thus, reacting $[Ru(L-L)_2(eilatin)]Cl_2$ with an excess of the appropriate $[Ru(L-L)_2Cl_2]$ precursor in ethylene glycol at 140 °C for 32 h yielded the corresponding dinuclear complex in good yields. We were able to monitor the progress of the reactions by UV−vis spectroscopy, following the appearance of a new low energy band around 750 nm and the disappearance of the typical MLCT band of the mononuclear eilatin complexes around 600 nm. The crude product was isolated as the hexafluorophosphate salt and purified by cation exchange chromatography using a column of Sephadex CM C-25 as support and a 5:3 mixture of MeOH and aqueous NaCl (in increasing ionic strength) as eluent. The unreacted mononuclear complexes eluted in a 0.1 M NaCl concentration, and the dinuclear species eluted by raising the ionic strength of the salt solution to 0.3 M.

Since the two metal centers of the dinuclear complexes are chiral and nonequivalent, we expected the formation of two diastereoisomeric pairs $\Delta\Delta/\Lambda\Lambda$ ("homochiral") and $\Delta\Lambda/\Lambda\Delta$ ("heterochiral"). ^{1}H NMR spectra of the crude reaction mixture and of the purified product revealed a 3:1 diastereoisomeric ratio determined as hetero/homo, respectively, by X-ray crystallography. We were able to isolate pure samples of both diastereoisomers by repeated crystallizations via slow evaporation of a toluene−acetonitrile solution of the diastereoisomeric mixture. The first batch consisted mainly of the less soluble heterochiral isomer which crystallized as square-shaped crystals, and a small amount of the homochiral isomer which crystallized as fine needles. The crystals were separated from the solution and recrystallized by the same method. X-ray quality crystals of the heterochiral isomers of both **4** and **5** were obtained in this manner. The mother liquor of the first crystallization trial was concentrated, and the solution was again allowed to slowly evaporate. An additional crop of the heterochiral isomer contaminated by a small amount of the homochiral isomer crystallized. The crystals were removed, and the solution was evaporated to afford an almost pure homochiral isomer as indicated by ^{1}H NMR spectra.

NMR Studies. The NMR characterization of the mononuclear complexes was accomplished as previously reported[8] utilizing ^{1}H COSY, NOESY, and HMQC two-dimensional NMR techniques. Mononuclear complexes of eilatin,[9] and of other large polyaromatic ligands,[5a−f] exhibit a strong dependence of the ^{1}H NMR chemical shifts on concentration and temperature. This phenomenon, which was also observed for compounds **2** and **3** of this study, is attributed to the formation of discrete dimers held by stacking interactions between the large aromatic eilatin moieties.

Upon the chelation of the "tail" binding site of eilatin by a second $[Ru(L-L)_2]^{2+}$ metal fragment in **2** and **3**, dinuclear species are formed (**4** and **5**, respectively). In contrast to **2** and **3**, the ^{1}H NMR spectra of the dinuclear complexes **4** and **5** are not concentration dependent. Thus, the large steric crowding imposed by the two metal centers essentially blocks

(18) Majumdar, P.; Falvello, L. R.; Tomás, M.; Goswami, S. *Chem. Eur. J.* **2001**, *7*, 5222.
(19) Paul, P.; Tyagi, B.; Bilakhiya, A. K.; Dastidar, P.; Suresh, E. *Inorg. Chem.* **2000**, *39*, 14.
(20) Fletcher, N.; Junk, P. C.; Reitsma, D. A.; Keene, F. R. *J. Chem. Soc., Dalton Trans.* **1998**, 133.

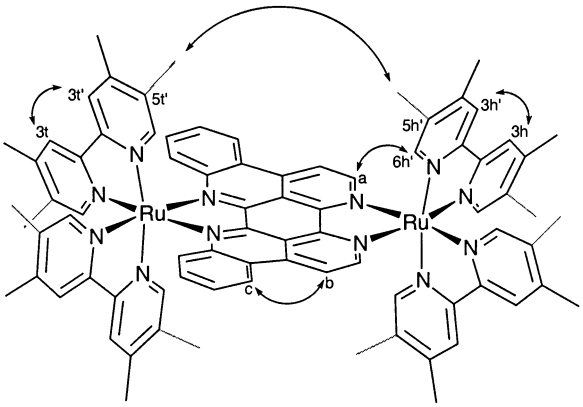

Figure 1. Heterochiral **4** and **5** (the additional methyl groups in **5** are shown in gray): numbering scheme and NOE correlations.

the space above and below the eilatin moiety, precluding any efficient stacking with an eilatin moiety of another complex. The NMR characterization of the dinuclear complexes was achieved by the same one- and two-dimensional NMR techniques applied for the mononuclear complexes. As an example, the characterization of heterochiral-**4**, which was isolated as already outlined, is described. The ^{1}H NMR reveals 18 resonances for 36 aromatic protons in accordance with the C_2 symmetry of this complex. The coupling pattern for each of the five different pyridyl rings and one benzo ring was assigned on the basis of COSY spectra. The connectivity between the two pyridyl rings of each dmbpy, and the connectivity between the pyridyl and benzo rings of eilatin was established by NOESY experiments (Figure 1). For each dmbpy, the H^3 proton shows an NOE to the adjacent $H^{3'}$ proton of the connected pyridyl ring in the same ligand. For eilatin, the H^b proton of the pyridyl ring shows an NOE to the adjacent H^c proton in the benzo ring. In addition, these NOESY experiments enabled us to determine which of the dmbpy ligands are bound to the "head"-Ru and which are bound to the "tail"-Ru: the H^6 and $H^{6'}$ protons of the two dmbpy fragments bound in the "head" of the complex showed a clear NOE connectivity to the H^a protons of eilatin. Moreover, the assignment of $H^{6'}$ and $H^{5'}$ protons on both ends of the complex, as those closer to the eilatin surface, could be established on the basis of their upfield location (0.2−0.4 ppm) compared to the respective H^6 and H^5 protons, due to strong ring currents arising from the eilatin fragment. Interestingly, a clear NOE correlation between the 5′-methyl groups of tmbpy in the "head" and "tail" ends of the analogous heterochiral-**5** complex indicated a close proximity between these groups (vide infra). Hence, a complete assignment and structure elucidation were accomplished for both **4** and **5**.

Crystal Structures. X-ray quality crystals of **3** were grown by the slow evaporation of a toluene−acetonitrile solution. Compound **3** crystallized as a racemate in a monoclinic unit cell of the *C*2/*c* space group, its structure resembling those of other eilatin containing mononuclear Ru(II) complexes for which a crystal structure was solved.[9] The asymmetric unit contains one molecule of the complex, two hexafluorophosphate ions, and one toluene molecule. The bond lengths (Table 1; Figure 2, left) of 2.04−2.07 Å between the nitrogens and the Ru(II) center are typical of bipyridyl-type ligands.[21] Both the tmbpy units and eilatin are not distorted substantially from planarity, indicating that the complex is unstrained. The unit cell contains 8 molecules of the complex with the eilatin moieties stacked face-to-face via the uncoordinated tail ends, forming discrete heterochiral dimers (Figure 2, right). The dimers feature an average interplanar separation of 3.4 Å, a typical distance for stacking interactions, with a Ru···Ru separation of 10.83 Å, similar to that observed for **6**.[9] Each dimer is separated from the next one (through the space above and below the eilatin moieties) by a toluene molecule.

Table 1. Selected Bond Lengths (Å) and Angles (deg) for $[Ru(tmby)_2(eilatin)[PF_6]_2$·toluene (**3**)

Ru−N(1)	2.068(4)
Ru−N(2)	2.044(4)
Ru−N(3)	2.062(4)
Ru−N(4)	2.060(5)
Ru−N(5)	2.073(5)
Ru−N(6)	2.074(5)
N(1)−Ru−N(2)	79.2(2)
N(3)−Ru−N(4)	79.2(2)
N(5)−Ru−N(6)	78.9(2)

Table 2. Selected Bond Lengths (Å) and Angles (deg) for ΔΛ/ΛΔ-[{$Ru(tmby)_2(\mu$-eilatin)$[PF_6]_4$·$4CH_3CN$·toluene (**5**)

Ru(1)−N(1)	2.071(5)	Ru(2)−N(3)	2.095(5)
Ru(1)−N(2)	2.058(5)	Ru(2)−N(4)	2.103(5)
Ru(1)−N(8)	2.059(5)	Ru(2)−N(5)	2.066(5)
Ru(1)−N(10)	2.078(5)	Ru(2)−N(6)	2.070(5)
Ru(1)−N(11)	2.060(5)	Ru(2)−N(7)	2.096(5)
Ru(1)−N(12)	2.061(5)	Ru(2)−N(8)	2.077(6)
N(1)−Ru(1)−N(2)	78.9(2)	N(3)−Ru(2)−N(4)	78.2(2)
N(9)−Ru(1)−N(10)	78.8(2)	N(5)−Ru(2)−N(6)	79.0(2)
N(11)−Ru(1)−N(12)	78.6(2)	N(7)−Ru(2)−N(8)	78.1(2)

The dinuclear complex **5** crystallized in a triclinic unit cell of the $P\bar{1}$ space group. Only one pair of enantiomers is present in the unit cell and was determined to be the heterochiral pair, ΔΛ/ΛΔ. Compound **4** crystallized in a monoclinic unit cell of the $P2_1/c$ space group. The asymmetric unit contains one heterochiral molecule of the complex, four hexafluorophosphate ions, and some disordered solvent molecules. The structure determination of **4**, which was derived from poor quality diffraction data, establishes the molecular structure and the stereochemistry of the complex. Since the structure of **4** resembles that of **5**, we will base the discussion on the structural parameters of the dinuclear complexes on the X-ray structure of **5**. The octahedral Ru(II) center at the "head" end of the bridging eilatin exhibits normal Ru−N bond lengths and the expected N−Ru−N bite angles (Table 2, Figure 3). However, the eilatin ligand is not fully planar, bending at the "tail" end, its structure reminiscent of the dibenzoeilatin ligand in the mononuclear complex $[Ru(bpy)_2(dbneil)]^{2+}$.[22] The conformation of the bridging eilatin is tilted with respect to the idealized equatorial plane of the octahedral ruthenium center at its "tail" end, probably due to steric interactions between

(21) Breu, J.; Stoll, A. J. *Acta Crystallogr., Sect. C.* **1996**, *52*, 1174.
(22) Bergman, S. D.; Reshef, D.; Groysman, S.; Goldberg, I.; Kol, M. *Chem. Commun*. **2002**, 2374.

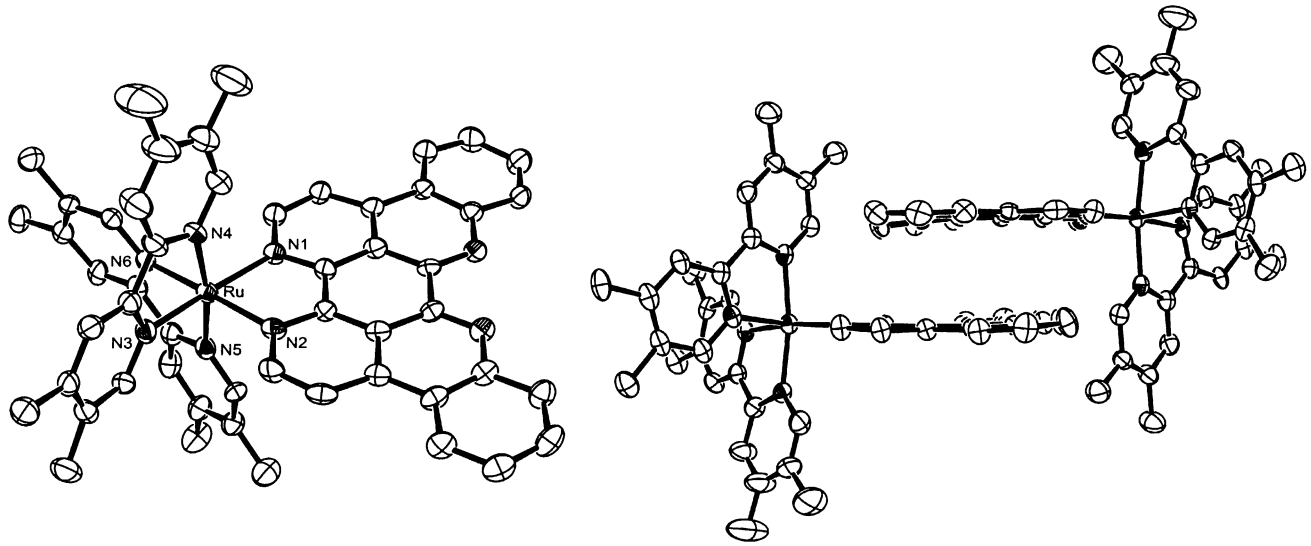

Figure 2. Left: ORTEP view (50% probability) of **3** featuring the "head"-bound eilatin, with labeling of key atoms. Right: A view of the dimer formed by Δ- and Λ-**3** in the unit cell, featuring the stacking interactions between the eilatin moieties. The eilatin fragment is not significantly distorted from planarity.

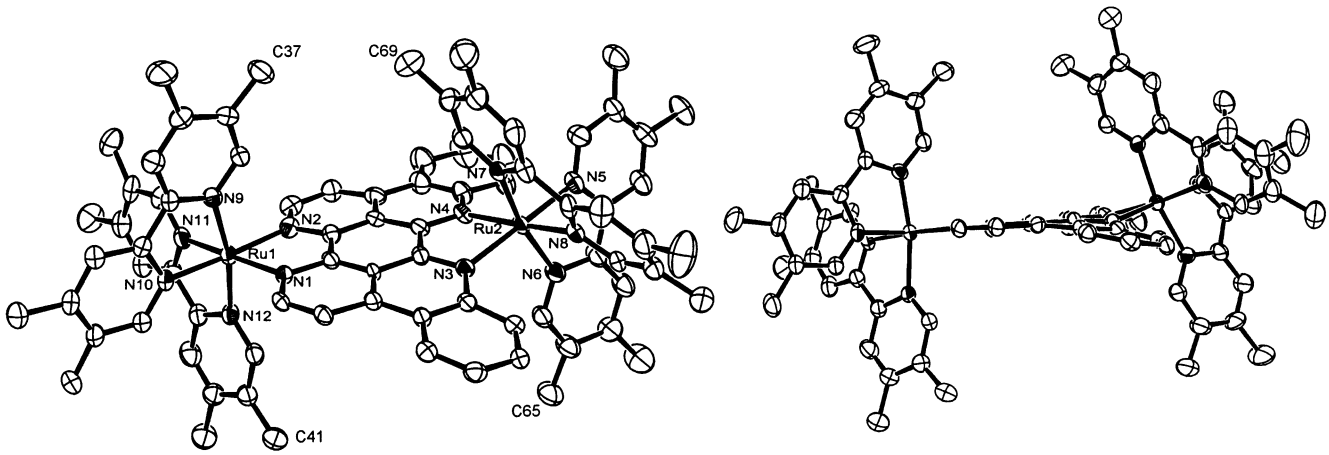

Figure 3. Left: ORTEP view (50% probability) of heterochiral **5** with labeling of key atoms. Right: Side view of **5** featuring the bending of the eilatin moiety at the "tail" end and the tilt of the Ru(II) center above it, placing the peripheral methyl groups on both ends in close proximity.

the eilatin and the peripheral tmbpy protons. These steric interactions are also proposed to be responsible for the slightly longer Ru−N bond lengths between the eilatin "tail" nitrogens and the metal center (2.10 Å) with respect to the "head" Ru−N bond lengths (2.07 Å). The tilt of the ligand positions the metal center slightly above the plane of the ligand situating the peripheral ligands of both ends in a closer range. Thus, the C(37)−C(69) distance between the nearest methyl groups of the tmbpy units above the eilatin plane is 3.91 Å, whereas the C(41)−C(65) distance between the analogous methyl groups below the eilatin plane is 7.85 Å. The metal−metal distance is 8.02 Å.

Absorption Spectra and Electrochemistry. The absorption spectra of **2**−**5** in acetonitrile are shown in Figure 4 in comparison to the spectrum of eilatin (**1**). Table 3 lists absorption maxima values and extinction coefficients of these complexes and that of the previously reported $[Ru(bpy)_2(eilatin)]^{2+}$ (**6**). It has been reported[19,23] that, for dinuclear complexes, stereochemistry may have an influence on the physical properties of the diastereoisomers. In the current study, no significant differences were observed in the spectral properties of the diastereoisomers; thus, the measurements were preformed on their mixtures.

The mononuclear $[Ru(L-L)_2(eilatin)]^{2+}$ complexes described in this work feature an intense dark green color (eilatin is bright yellow). The absorption spectra of these complexes exhibit intense bands in the UV region (200−350 nm), assigned to ligand-centered $\pi \rightarrow \pi^*$ transitions. The visible region is characterized by moderately intense bands (350−500 nm) assigned to eilatin-centered $\pi \rightarrow \pi^*$ transitions and to $d_\pi(Ru) \rightarrow \pi^*$ (L−L) metal-to-ligand charge transfer (MLCT) transitions, as well as a unique low energy broad $d_\pi(Ru) \rightarrow \pi^*$ (eilatin) MLCT transition at ca. 600 nm due to the low lying π^* orbital of eilatin. The mononuclear complexes are only weakly emissive at room-temperature.

The two dinuclear eilatin complexes feature an intense yellow-green color. The absorption spectra of the dinuclear species retain most of the features of the mononuclear

(23) (a) Kelso, L. S.; Reitsma, D. A.; Keene, F. R. *Inorg. Chem.* **1996**, *35*, 5144. (b) Rutherford, T. J.; Van Gijte, O.; Kirsch-De Mesmaeker, A.; Keene, F. R. *Inorg. Chem.* **1997**, *36*, 4465. (c) Browne, W. R.; O'Connor, C. M.; Villani, C.; Vos, J. G. *Inorg. Chem.* **2001**, *40*, 5461

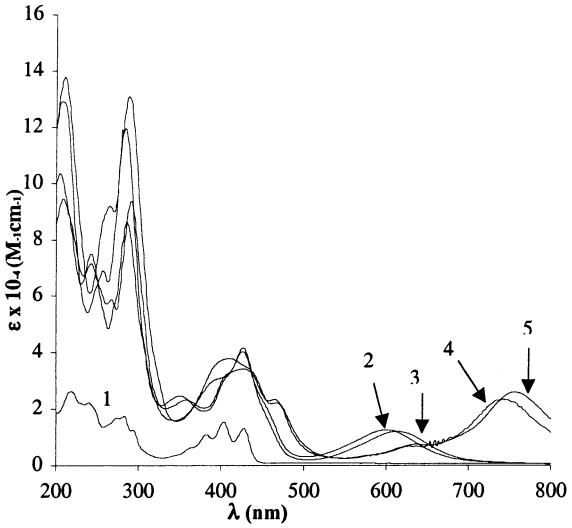

Figure 4. Absorption spectra of eilatin (**1**), $[Ru(dmbpy)_2(eilatin)][PF_6]_2$ (**2**), $[Ru(tmbpy)_2(eilatin)][PF_6]_2$ (**3**), $[\{Ru(dmbpy)_2\}_2(\mu\text{-eilatin})][PF_6]_4$ (**4**), and $[\{Ru(tmbpy)_2\}_2(\mu\text{-eilatin})][PF_6]_4$ (**5**) in acetonitrile solution, at room temperature.

Table 3. Spectral Data

compd	absorption maxima λ_{max}, nm ($\epsilon \times 10^{-4}$, M^{-1}, cm^{-1})
1[a]	242(4.8), 286(3.7), 360(1.1), 388(2.1), 408(3.0), 434(2.7)
1[b,c]	240, 283, 360, 382, 404, 428
6[b]	241(6.8), 286(7.3), 341(2.2), 405sh, 424(3.3), 460sh, 583(1.0)
2[b]	243(7.3), 286(8.6), 350(2.4), 403sh, 426(4.0), 460sh, 601(1.2)
3[b]	272(7.1), 267(5.9), 291(9.4), 358(2.3), 403sh, 427(4.2), 613(1.2)
4[b]	256(6.9), 284(12.0), 396(sh), 428(3.4), 466(2.3), 628(0.7), 740(2.4)
5[b]	265(9.2), 288(13.1), 410(3.8), 430(sh), 467(2.2), 636(0.7), 755(2.6)

[a] From ref 7 in methanol. [b] In acetonitrile. [c] Due to the low solubility of **1** in acetonitrile, only the wavelengths for the absorption maxima are given.

complexes, namely, intense bands in the UV region and two distinct broad bands in the visible region. However, a few differences are apparent: the dinuclear species exhibit higher extinction coefficients in the UV range; the absorption bands in the 350−500 nm region span across a wider range and are somewhat less intense; and, most significantly, a striking 140 nm red shift of the $d_\pi(Ru) \rightarrow \pi^*$ (eilatin) MLCT transition is observed, from λ_{max}= 601 nm in **2** to 740 nm in **4** and from 613 nm in **3** to 755 nm in **5**.

Cyclic and square wave voltammetry methods were used to determine the redox behavior of complexes **2**−**6** in acetonitrile. Due to the low solubility of eilatin, its redox behavior was not explored. $E_{1/2}$ values for successive closely spaced reduction processes were determined using the peak potential value (E_p) from the square wave measurements. The results are summarized in Table 4. The results obtained under the same conditions for $[Ru(bpy)_3]^{2+}$ are also shown for comparison purposes.

The mononuclear complexes **2**, **3**, and **6** displayed one metal-centered oxidation ($Ru^{III/II}$), and successive one-electron reductions of the ligands, all of which appeared to be reversible redox processes (Figure 5).[24] Their one-electron nature is evident from their current intensities in the oxidation and reduction square wave voltammograms. Interestingly, the first reduction process, is apparently split into two separate waves each exhibiting half the current intensity of the following reduction waves and of the oxidation wave.[25]

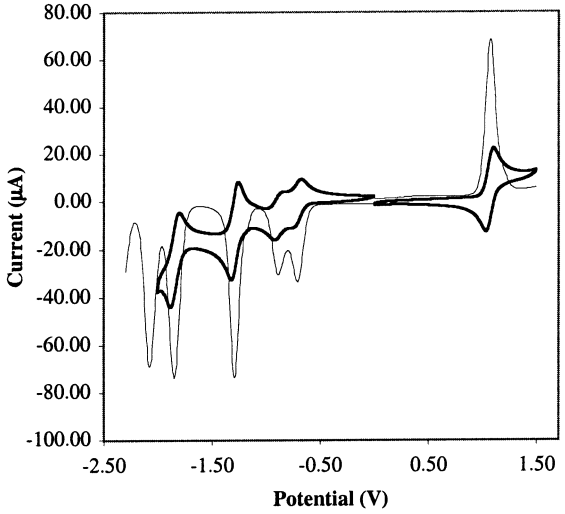

Figure 5. Cyclic and square wave voltammograms of **6** (recorded in acetonitrile, vs $Ag/AgNO_3$), featuring the splitting of the first reduction wave.

The first two reduction processes in **2**, **3**, and **6** occur at potentials significantly anodically shifted with respect to those of $[Ru(bpy)_3]^{2+}$ and are attributed to two consecutive reductions of eilatin, demonstrating that eilatin is a much better π-accepting ligand than the bpy-type ligands. The following reduction processes occur at potentials reminiscent of those of $[Ru(bpy)_3]^{2+}$. The oxidation potential of the metal center in $[Ru(bpy)_2(eilatin)]^{2+}$ (**6**) is anodically shifted with respect to that of $[Ru(bpy)_3]^{2+}$ (1.38 V vs 1.28 V vs SCE, respectively). Replacing the bpy ligands in **6** with dmbpy to give **2** causes a cathodic shift in the oxidation potential of the $Ru^{III/II}$ process by 0.09 V, and a further cathodic shift of 0.06 V is observed on going from **2** to **3**. In comparison, the reduction potentials are affected to a lesser extent by the additional methyl substituents (Table 4).

The dinuclear complexes **4** and **5** show two well-resolved and reversible metal-centered oxidations, the first in each occurring at a potential ca. 0.03 V more anodic than the first oxidation potentials of **2** and **3**, respectively (Figure 6). The second oxidation wave is anodically shifted by 0.30 V relative to the first for both **4** and **5**. Both complexes undergo two reversible reductions, attributed to the two successive one-electron reductions of the bridging eilatin, the first

(24) A square wave voltammogram of compound **6** which seemed to be somewhat contaminated (as evident from the presence of an extra reduction wave) was recently described: Glazer, C. E.; Tor, Y. *Angew. Chem., Int. Ed.* **2002**, *41*, 4022.

(25) This phenomenon could stem from dimerization of the eilatin complexes via $\pi-\pi$ stacking, as it was also observed for other mononuclear eilatin complexes that exhibit a *strong* tendency to dimerize in solution. Namely, the first reduction process does not represent a one-electron reduction of a monomeric species, but rather two consecutive one-electron reductions of a dimeric species, hence the half current intensities. Addition of electrons lowers the stacking tendency; thus, the following reduction waves are attributed to monomeric species. Consistently, upon gradual dilution of the mononuclear complexes, the splitting of the first reduction wave diminishes. In addition, dinuclear complexes **4** and **5** (that do not stack in solution) did not exhibit this phenomenon and displayed two one-electron reversible eilatin-centered reduction waves. Other compounds for which substantial stacking interactions were reported did not exhibit this trend.[5a−f,26] We are currently investigating the source of this phenomenon.

Table 4. Half Wave Potentials for the Oxidation and the Reduction of the Complexes[a]

compd	Ru(III/II)	E_{red1}		E_{red2}	E_{red3}	E_{red4}
$[Ru(bpy)_3]^{2+}$	1.28	−1.33		−1.53	−1.78	
6	1.38 (70)	−0.40 (60)	−0.59 (60)	−0.99 (60)	−1.54 (60)	−1.78[b]
2	1.29 (60)	−0.43 (60)	−0.61 (60)	−1.01 (60)	−1.64[b]	−1.86[b]
3	1.23 (60)	−0.47 (60)	−0.65 (60)	−1.03 (70)	−1.80[b]	
4	1.31 (70), 1.61 (60)	−0.07 (70)		−0.56 (70)	−1.56[c]	
5	1.26 (70), 1.56 (70)	−0.10 (70)		−0.60 (70)	−1.72[c]	

[a] Potentials are given vs SCE in acetonitrile, with 0.1 M Bu_4NPF_6 as supporting electrolyte, measured at room temperature with scan rate of 0.1 V/s, ΔE_p values in mV given in parentheses. [b] Values determined from square wave voltammetry. [c] Unresolved processes.

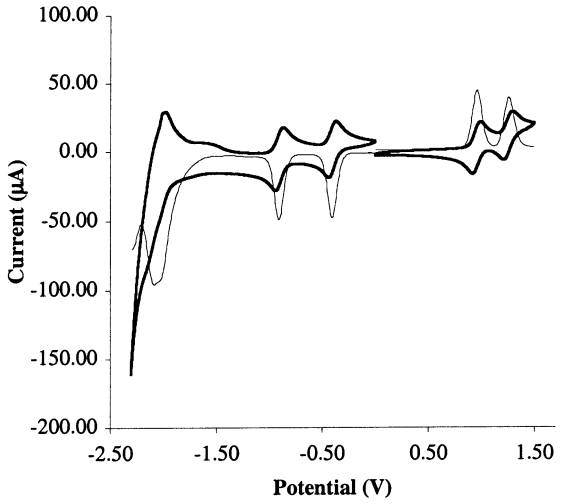

Figure 6. Cyclic and square wave voltammograms of **5** (recorded in acetonitrile, vs $Ag/AgNO_3$).

occurring at a substantially anodically shifted potential (ca. 0.36 V shift) compared with the first wave (of the split process) in the mononuclear analogues, and it is not split.[25] Subsequent reduction processes, associated with the reduction of the peripheral bpy-type ligands, are also anodically shifted with respect to the mononuclear analogues, but to a lesser extent and are ill-behaved (unresolved).

Discussion

Syntheses and Structure. The common method for the synthesis of mononuclear complexes of the $[Ru(L-L)_2(BL)]^{2+}$ (BL = bridging ligand) type consists of the reaction of a slight excess of the bridging ligand with the appropriate building block. This method usually produces some amount of the dinuclear species,[27] which may be difficult to remove. The nonequivalent nature of the two binding sites in eilatin affords the selective formation of the "head"-bound mononuclear complexes, if relatively mild reaction conditions are applied. To further react the second chelating "tail" site, more drastic conditions are necessary, and thus, both the mono- and dinuclear complexes bridged by eilatin could be synthesized in high selectivity and in good yields.

The preparation of the dinuclear complexes **4** and **5** affords the two diasteroisomeric pairs, $\Delta\Lambda/\Lambda\Delta$ and $\Delta\Delta/\Lambda\Lambda$ in a 3:1 ratio, respectively. In general, a statistical distribution of the heterochiral and homochiral forms is expected, and in many reports, where quantification of the diastereoisomeric ratio could be made, that is indeed the case.[6c,20,23b,28] There are a few exceptions however, where a preference toward the formation of the heterochiral (or *meso*) diastereoisomer was reported.[23a,29] In one case,[23a] the possible explanation for the heterochiral preference was based on the examination of a model of the homochiral form, which revealed possible interligand interactions. In the current work, the X-ray structures of **4** and **5** may provide a possible explanation. The tilt of the bridging eilatin positions the metal center at the tail end slightly above the plane of the ligand. Although the metal−metal separation is virtually unchanged,[30] the tilting of the octahedral center situates the peripheral ligands of both ends in a closer range. This could bring about significant interligand interaction and account for the heterochiral preference. In solution, the dinuclear complexes feature a C_2-symmetry, implying a fast wagging motion of the "tail" end on the NMR time scale.

Absorption Spectra and Electrochemistry. The absorption spectra of mononuclear complexes **2** and **3** exhibit similar features to those of previously reported mononuclear eilatin containing Ru(II) complexes. The addition of methyl substituents to terminal polypyridyl ligands raises the energy of the d_π(Ru) orbital and consequently lowers the energy of the $d_\pi(Ru) \rightarrow \pi^*$ (eilatin) MLCT transition.[31] Therefore, a clear red shift of the absorption maximum of the low energy MLCT is observed on going from **6** (583 nm) to **2** (601 nm) and further on to **3** (613 nm).

The coordination of an additional chromophoric $[Ru(L-L)_2]^{2+}$ unit to the "tail" end leads to the formation of dinuclear complexes and brings about several changes in the absorption spectra. The higher extinction coefficients in the UV range, associated with intense ligand centered $\pi \rightarrow \pi^*$ transitions, are attributed to the increase in the number of the chromophoric units. The coordination of the second electron-withdrawing metal fragment is also expected to affect the energy levels of the complex, thereby changing the energy of the transitions. Mainly, the π^* level of eilatin and the d_π level of the Ru(II) are expected to be stabilized. Electrochemical data (vide infra) support a slight stabilization of the d_π(Ru) orbital and a significant stabilization of the

(26) Campagna, S.; Serroni, S.; Bodige, S.; MacDonnell, F. M. *Inorg. Chem.* **1999**, *38*, 692.
(27) Ernst, S. D.; Kaim, W. *Inorg. Chem.* **1989**, *28*, 1520.
(28) Hua, X.; Von Zelewsky, A. *Inorg. Chem.* **1995**, *34*, 5791.
(29) (a) Wu, F.; Riesgo, E.; Pavalova, A.; Kipp, R. A.; Schmehl, R. H.; Thummel, R. P. *Inorg. Chem.* **1999**, *38*, 5620. (b) Baitalik, S.; Florke, U.; Nag, K. *Inorg. Chem.* **1999**, *38*, 3296.
(30) The same M−M distance was reported for the bridging phenanthroline-5,6-diimine[6c] (BL), in which the two binding sites are at the same distance apart as in eilatin. In the X-ray structure of $[\{Ru(bpy)_2\}_2(\mu\text{-}BL)]^{4+}$, the bridging ligand is not tilted with respect to the idealized octahedral plane, and both metal centers are not substantially distorted.
(31) Anderson, P. A.; Strouse, G. F.; Treadway, J. A.; Keene, R. F.; Meyer, T. J. *Inorg. Chem.* **1994**, *33*, 3863.

π^*(eilatin) orbital. Although several absorptions are expected to shift in the 350−500 nm region, e.g., a blue shift of the d_π(Ru) → π^*(L−L) transition, the overall absorption in this region is hardly affected, being slightly broadened. The dramatic red shift in the d_π(Ru) → π^*(eilatin) MLCT transition on going from the mononuclear to the dinuclear complexes results from the stronger stabilization of the LUMO level relative to the HOMO level, thus reducing the energy gap between them. The intensity of the low energy MLCT band in the dinuclear complexes is double that of the mononuclear complexes in accordance with an additional metal-based $[Ru(L-L)_2]^{2+}$ chromophore unit. The two different binding sites of the bridging eilatin may lead to two different d_π(Ru) → π^*(eilatin) MLCT transitions; however, this difference is apparently too small, as only one broad MLCT band is observed. The methyl substituents on the L−L ligands play the same role in the dinuclear complexes as observed for the mononuclear ones, leading to a 15 nm red shift in **5** relative to **4**. Further support for this interpretation is given by the electrochemical studies.

Keene, Meyer, and co-workers[31,32] have shown that it is possible to design black MLCT absorbers by utilizing electron-withdrawing polypyridyl ligands with a low π^* orbital on one hand, and electron-donating ligands to stabilize the "hole" at the Ru^{III} center in the MLCT state, on the other. Both mono- and dinuclear complexes of eilatin with Ru(II) fall into that category, exhibiting absorption spectra which cover most the visible spectral range and up to the near-IR region.

The electrochemical properties of all of the mononuclear eilatin complexes are consistent with their absorption spectra. Most significantly, the low energy MLCT transition attributed to d_π(Ru) → π^*(eilatin) is in good accordance with the substantially anodically shifted first reduction process attributed to the reduction of eilatin. The strong π-accepting character of eilatin also affects the oxidation process by the stabilization of the d_π(Ru) orbital. In contrast, the electron donating methyl substituents on the bpy-type ligands destabilize the d_π(Ru) orbital causing a cathodic shift in the oxidation potential in **2** and **3** relative to **6**.

As previously discussed, the addition of a $[Ru(L-L)_2]^{2+}$ subunit to the second coordination site of eilatin results in a net stabilization of the π^*(eilatin) and of the d_π(Ru) orbitals. Consequently, anodic shifts of both the first metal-based oxidation and the first ligand-based reduction (compared with the mononuclear analogues) are expected and are indeed observed. The splitting of the metal-centered oxidation processes observed for the dinuclear species ($\Delta E = E_{ox1} - \Delta E_{ox2} = 0.3$ V for both **4** and **5**) may be attributed to the nonequivalence of the two coordination sites of eilatin and/or to a significant electronic interaction between the metal centers.[33] For identical ligand-bridged metal centers (with a symmetrically bridging ligand), the extent of the splitting indicates the degree of the metal−metal interactions.[34] Preliminary results obtained for the redox properties of the related dinuclear complex $[\{Ru(bpy)_2\}_2(\mu\text{-dbneil})]^{4+}$ (dbneil = dibenzoeilatin) with the symmetrical bridging ligand dbneil[35] indicated a weaker, yet significant ($\Delta E = 0.17$ V), metal−metal interaction. Thus, we conclude that the difference between the two metal-centered oxidation processes in **4** and **5** is a result of both the communication between the metal centers as well as the nonequivalency of the binding sites. The metal−metal interaction via the bridging ligand eilatin may be explained on the basis of superexchange theory,[34] where the overlap between metal orbitals is mediated via those of the bridging ligand. The metal−metal communication in these dinuclear complexes is enabled by an electron transfer process via the low lying π^* orbital of the bridging eilatin.

Conclusion

We have shown the selective synthesis of both mono- and dinuclear complexes with the nonequivalently bridging ligand eilatin. The dinuclear complexes formed in a 3:1 hetero- to homochiral diastereoisomeric ratio, attributed to the close proximity of the peripheral ligands. The strong π-accepting character of eilatin combined with the electron-donating character of tmbpy and dmbpy leads to unique low energy MLCT transitions, and to dramatically anodic eilatin-centered reduction potentials for both the mono- and the dinuclear complexes. The electronic communication observed between the two metal centers in the dinuclear complexes is proposed to be mediated by the low lying π^* orbital of the bridging eilatin. The extent of the metal−metal communication in these complexes may be evaluated by the comparison between the oxidation potentials of the homodinuclear Ru−Ru, Os−Os and heterodinuclear Ru−Os, Os−Ru complexes, as was described in other studies with nonsymmetric bis chelating ligands.[6a,b] We are currently exploring the degree of interaction between the metal centers in eilatin-bridged complexes.

Acknowledgment. This research was supported by the Israel Science Foundation founded by the Israel Academy of Sciences and Humanities. We thank Sheba D. Bergman for a sample of $[\{Ru(bpy)_2\}_2(\mu\text{-dbneil})][PF_6]_4$ and Dvora Reshef for technical assistance.

Supporting Information Available: X-ray crystallographic files in CIF format for the structure determinations of complexes **3**, **4**, and **5**. This material is available free of charge via the Internet at http://pubs.acs.org.

IC020703C

(32) Anderson, P. A.; Keene, F. R.; Meyer, T. J.; Moss, J. A.; Strouse, G. F.; Treadway, J. A. *J. Chem. Soc., Dalton Trans.* **2002**, 3820.

(33) A possible approach to gain insight on which metal center is easier to oxidize would be to compare the electrochemical properties of the relevant mononuclear complexes, e.g., $Ru[(bpy)_2(head\text{-}eilatin)]^{2+}$ and $[Ru[(bpy)_2(tail\text{-}eilatin)]^{2+}$; however, the latter cannot be synthesized. A complex which resembles the latter to some extent is $[Ru(bpy)_2(dbneil)]^{2+}$.[22] This complex is oxidized in a more positive potential relative to $[Ru(bpy)_2(head\text{-}eilatin)]^{2+}$, which may suggest that the ruthenium bound to the head-site of eilatin would be oxidized first in the bimetallic complexes.

(34) See, for example, ref 1a,b and references therein.

(35) Bergman, S. D. Unpublished results.